PHYSICAL REVIEW B **79**, 161404(R) (2009)

Transport in a metallic nanotube at finite temperature

Wei Ren,[1,*] Cai-Zhuang Wang,[2] Kai-Ming Ho,[2] and C. T. Chan[1]
[1]*Department of Physics, The Hong Kong University of Science and Technology, Hong Kong, China*
[2]*Ames Laboratory-USDOE, Iowa State University, Ames, Iowa 50011, USA*

(Received 21 November 2008; revised manuscript received 9 March 2009; published 27 April 2009)

We consider the effect of thermal phonon displacements on the coherent transport in carbon nanotubes. The atomic displacements are generated using tight-binding molecular dynamics simulations, and the conductances are computed using a nonequilibrium Green's function technique. Atomic displacements due to lattice vibrations lead to different levels of conductance reduction and fluctuation on the massive and massless bands of a metallic nanotube. Different conduction regimes are studied by examining the resistance on different length scales. The temperature-induced displacements have a significant impact on the ballistic or diffusive transport in carbon nanotube.

DOI: 10.1103/PhysRevB.79.161404 PACS number(s): 73.63.−b, 63.22.−m, 65.80.+n

Resistive heating is expected to be a severe problem when the miniaturization of electronic components reaches the ultimate limit of the nanoscale. Such an overheating effect is unavoidable for nanowire made of the ordinary metals or *III-V* semiconductors. As a potentially ballistic conductor,[1] carbon nanotubes seem to offer a unique alternative conducting wires and elements. This is a result of their peculiar band dispersion and absence of surface scattering for conduction electrons. On the other hand, there must be a transition from ballistic to diffusive transport and eventually to localization behavior in a one-dimensional system when disorder sets in. The question is about the length of the tube and the amount of disorder that will make such transitions observable. We present results of electron transport for carbon nanotube segments of different lengths in the presence of different amount of atomic position disorder, owing to the finite temperature-induced lattice vibrations. The atomic displacements are generated using the tight-binding molecular dynamics (TBMD). The impact of lattice distortions on the charge transport is captured by the configurational averaging statistics. In this scheme, electron-phonon interactions for a large number of vibrational modes in realistic nanotubes need not be directly calculated.[2] In contrast, so far calculations of electron-phonon matrix element calculations have been limited to study periodic nanotube or small molecular systems.[3]

The model structure is an armchair metallic (6,6) nanotube which consists of 576 carbon atoms in the scattering region ($d \sim 60$ Å in length). To better deal with the low frequency acoustic and optical phonon modes an even longer tube supercell could be considered, although that makes our computation more expensive. First, we run TBMD (Ref. 4) at 100, 300, and 700 K, where the temperature has been rescaled to take zero point motion into account. The details of the TBMD method can be found elsewhere.[5,6] The advantage of the TBMD approach is that it incorporates the electronic effects into molecular dynamics (MD) through an environment-dependent tight-binding Hamiltonian,[7,8] with parameters fitted to a very broad data generated by first-principles calculations. We have calculated some phonon frequencies of diamond and graphene structures at some selected zone boundary points using this environment-dependent TB model and compared the results with experiments very well. It can obtain structural and phononic properties with an accuracy that is comparable to first-principles calculations but with much less computation resources. The temperature-dependent anharmonic effects are automatically included in the lattice vibration properties. We let the system reach equilibration, and the atomic configurations for 300 snapshot frames were then extracted from 3000 MD steps at a specific temperature. For each of these configurations, we calculate the linear response conductance $G(E)=g(E)2e^2/h$ where the transmission $g(E)$ is calculated by Green's function and Landauer formula.[9] The calculated conductance has been be averaged over the ensemble of 300 configurations. Two perfect semi-infinite (6,6) nanotube electrodes were connected to our vibration scattering region by transparent intratube contacts.[10] To include the effect of temperature in the conductance, we have $G(T)=\frac{2e^2}{h}\int_{-\infty}^{\infty} g(E)(-\frac{\partial f}{\partial E})dE$ where $f=1/(e^{(E-E_f)/k_BT}+1)$ is the Fermi-Dirac distribution function. Essentially this is a convolution of the conductance and the thermal smearing function $-\frac{\partial f}{\partial E}=\frac{1}{4k_BT}\sec h^2(\frac{E}{2k_BT})$ which averages the zero-temperature conductance over an energy range of k_BT. The covalent-bond length dependent Hamiltonian matrix elements are computed by the transferable tight-binding potential. We introduce no impurity or vacancy defect[11] scatterers in the whole carbon network, and thus solely the lattice disorder comes from the displacements due to the thermal phonons. The change in conductance is due to the scattering effect of the "frozen" phonons as a result at a particular temperature. In experimental situations, the defect disorder effect[12] will superimpose on the phonon effect and may play an important role in the low-temperature regime. Our approach is based on solving a stationary Schrodinger equation, assuming adiabatic approximation to be validated.[13] At this point, we should spell out the limitation of the present approach, which treats the effect on the resistance of nanotubes due to thermal phonons by considering the effect of lattice displacement on transport. In the case of static disorder of atomic coordinates, the spatial localization of electron wave functions is the consequence of the interference effect of multiple scattered electron waves. In a dynamical situation, the mechanism is much more complicated. For example, dynamical scattering events can lead to complexities such as dephasing due to inelastic scattering, phonon-assisted tunneling, phonon induced nonequilibrium

 ©2009 The American Physical Society

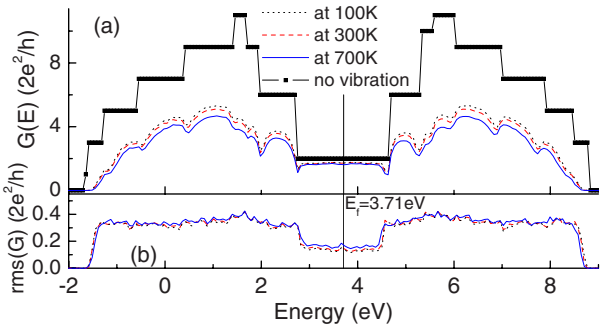

FIG. 1. (Color online) (a) One segment of vibrated metallic nanotube (length: $d \sim 60$ Å) carries suppressed average conductance especially for higher-energy states, while less affected for linear band near Fermi energy $E_f=3.71$ eV. The ideal ballistic nanotube has quantized resistance of $1/2G_0=h/4e^2=6.45$ kΩ. (b) The fluctuations of average conductances in (a) show different behaviors near and away from Fermi level. We can also observe that the higher the temperature, the smaller (larger) the average conductance (conductance fluctuation) is.

gap opening.[14–16] These phenomena, which will affect transport, cannot be captured in the present static approach. The effect of nonadiabatic effects on electron dynamics in the presence of moving nuclei is beyond the scope of this work. Acoustic phonon is operative in our investigation, while we have restricted ourselves to the low applied bias regime coherent transport. Therefore the optical phonon limited high-field mobility of carbon nanotubes is not accessible with this methodology.

In Fig. 1(a), we compare the averaged conductance at 100, 300, and 700 K (over 300 configurations) with the ballistic conductance for an ideally periodic nanotube without phonon displacements, where the conductance is independent of the sample length. This is the ideal ballistic transport for the nanowire which does not follow the Ohm's law.[10] However temperature introduces atomic displacements and significant backscattering for electronic states far away from the Fermi level E_f while having only minimal effects on the linear bands crossing at E_f. This effect roots in the fact that only two bands of different symmetries contribute to transport near Fermi level,[17] and the special topological properties of the dispersion near the Dirac point protects the system from backscattering between one band and the other at the same K point. Although $K \rightarrow K'$ backscattering is allowed, the long-range atomic displacement due to phonons is very insufficient in causing such large momentum transitions. But these arguments do not apply to other bands, and the effect of atomic displacement on scattering is much higher. From Fig. 1(a) conductance dips at subband edges are also observed, when a new set of states across the threshold starts to contribute. At the higher subbands, a lot more backscatterings can take place and the transport behavior will then become diffusive in those energies.

The sample-to-sample variation in conductance is also an important piece of information about the conductive properties of nanotubes. The universal conductance fluctuation (UCF) (Refs. 18 and 19) behavior in quasi-one-dimensional systems can be observed on the higher-energy massive bands of the nanotube. This UCF value of 0.365 $(2e^2/h)$ again shows a diffusive transport characteristic in the higher-energy bands at the specific temperature. But for the massless linear band near Fermi point, the UCF prefactor value is remarkably suppressed by nearly one-half. In another independent work based on random on-site potential disorder model, we have actually overlooked this distinctive feature (see Fig. 1 of Ref. 9). Figure 1(b) shows the root-mean-square (rms) $(G=[\langle G^2\rangle-\langle G\rangle^2]^{1/2})$ values of the averages in Fig. 1(a). At first sight, the rms reduction value by a factor of 2 seems to coincide with the characteristic of symplectic symmetry for the linear band of carbon nanotube. Corresponding to Dyson's classification of orthogonal, unitary and symplectic symmetry classes, the UCF values have been discovered to be $\sqrt{2/15\beta}$, where $\beta=1$, 2, and 4, respectively. An interesting question to ask is that whether this reduction reflects the genuine symplectic universality. If so, should it be independent on many parameters? We have compared the fluctuations of the two different energy regions: one near and one far away from the Dirac point as a function of tube length and as a function of disorder. We found that the UCF values reaches 0.365 $(2e^2/h)$ very quickly for energies far away from the Dirac point. For energies near the Dirac point, the UCF value is *length dependent* and will increase to 0.365 $(2e^2/h)$ for a sufficiently long tube, and thus, this value seen in Fig. 1(b) is just an intermediate behavior before the conventional UCF shows up for a much longer nanotube or equivalently stronger disorder. In other words, this merely manifests the fact of robust quasiballistic transport at the nanotube Fermi level within a weakly disordered regime. As we increase the nanotube length, we find that the "symplecticlike" fluctuation will cross over to the normal UCF value.[20] The conductance fluctuation value from the linear bands will rise as the tube length increases and eventually level off at the normal UCF value. Interestingly very recently the suppression of conductance fluctuation in the mesoscopic graphene samples near the charge neutrality point has been reported.[21]

We see that near E_f, the intrinsic conductance of nanotube only degrades slightly at room temperature or even up to 700 K. This weak temperature dependence behavior is crucial for the applications of nanotubes as metallic quantum wire. From the bond length statistics in Fig. 2, different temperatures lead to different structural disorders and, thus, to the fluctuations of hopping energies in tight-binding model. The equilibrium carbon-carbon atom distances are single valued at 1.42 Å for the nearest neighbors, 2.46 Å for the second nearest neighbors, and 2.84 Å for the third (vertical lines in Fig. 2). In particular, we observe that the lengths of double ($r=1.31$ Å), conjugated ($r=1.42$ Å), and single ($r=1.54$ Å) bonds are all present in the radial distribution function.[22] The radial distribution functions are all broadened increasingly as temperature goes up, with a corresponding decrease in height. Anyhow these dependences are relatively insignificant since carbon has a very high Debye temperature. We also note that the peaks in radial distribution function are not symmetrically distributed due to anharmonicity contribution captured in our TBMD scheme.

To consider the disorder effect on tubes of increasing lengths, we randomly interconnect different segments of MD generated nanotube atomic coordinates to form longer tubes

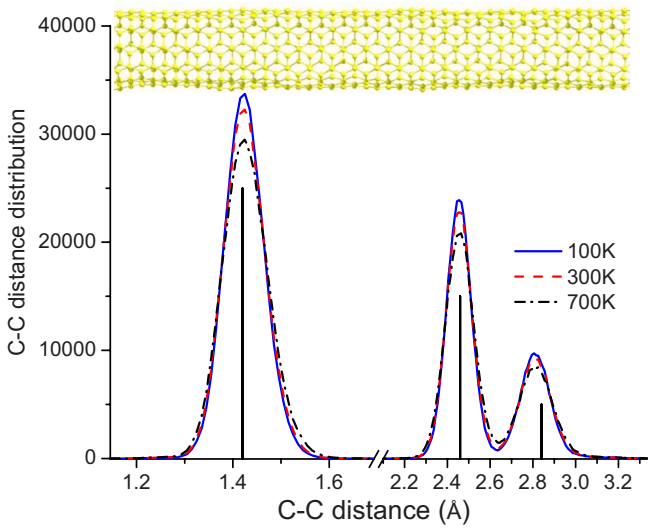

FIG. 2. (Color online) Inset shows the displaced schematic configurations at room temperature, which gives the carbon-carbon distances broadened in the histogram. In the main frame three vertical lines indicate the first, second, and third nearest-neighbor distances for the perfect equilibrium configuration. The cutoff distance of electron overlapping in our tight-binding model is 3.3 Å.

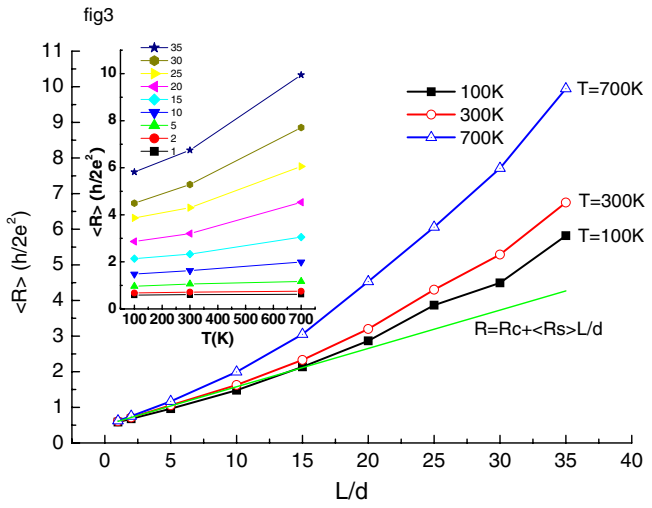

FIG. 3. (Color online) Calculated resistance scalings of long nanotubes under different temperatures are shown. The green solid line shows the resistance for Ohm's law behavior with linear length dependence. The inset displays the same data set but now as a function of temperature for different number of interconnected segments.

to study the transport scaling. This strategy is the same as a recent study on the doped silicon nanowires.[23] Our coalescent longest nanotube is composed of 20 160 carbon atoms. In the calculation of conductance near the Fermi energy, a statistical average has been done over 300 coalescence realizations for each tube length. The results are shown in Fig. 3 in which we give the ensemble-averaged resistance as a function of tube length for atomic configurations generated at three different temperatures. If the electron transport is ballistic, the resistance should not depend on length. However, we found that the resistances grow as functions of length. It initially increases in a linear manner, indicating that the length of the tubes we considered is in the quasiballistic or diffusive regime. In such a regime, as the resistance is commonly analyzed with a linear relation in the form $R=R_c+\langle R_s\rangle L/d$, where $R_c=1/G_0=(1/N)h/2e^2$ is contact resistance, $\langle R_s\rangle$ is resistance of a single segment, and L/d is the segment repeating number. If we take the mean-free path as the distance in which the resistance has become twice the value of the intrinsic contact resistance, the mean-free path is about 300 Å. For the even longer nanotube, the resistance starts to increase more rapidly above the initial linear scaling behavior, manifesting the so-called medium localization.[24] Eventually the resistance should increase exponentially or superlinearly with length when one-dimensional localization effect emerges, as confirmed in the recent experiment.[25] Further we can observe that as the temperature increases, the deviation from single segment linear scaling becomes larger and the onset length scale for localization is reduced. We have fitted the data with a power-law relation $R=a(L/d)^b$ and found the exponent b values to be 1.10, 1.15, and 1.33 for 100, 300, and 700 K, respectively. For a given tube length, the intrinsic resistance of the freestanding one-dimensional metallic nanotube is found to increase with the absolute temperature.[26] As the tube length increases, temperature starts to play a more dominant role, and the atomic displacements eventually cause localization effect to set in. This thermal effect is more clearly presented in the inset of Fig. 3 where we replot the scaling data in the main frame. For the longest tube $L/d=35$ considered here, we can estimate the temperature coefficient to be about $\alpha=(1/R)dR/dT\simeq 0.001/\mathrm{K}$.

In conclusion, the quantum conductance in a metallic freestanding single-wall nanotube is studied at several temperatures. Substantial temperature dependence of the conductance in the range of 100–700 K has been revealed. We show that at a specific temperature the atomic displacements induce scattering, which in turn impose a length scale for ballistic transport along the metallic nanotube. Our method can be applied to investigate other carbon materials such as graphene where buckling effect is also important at room-temperature condition.[22]

Recently, experimental work has been carried out to measure the individual metallic single-wall carbon nanotube's resistance from room temperature up to 1000 K in vacuum. A relatively small linear temperature dependence of resistance is obtained.[27] Their measured temperature coefficient $1.1\times 10^{-3}/\mathrm{K}$ is in good agreement with our long nanotube calculations. This value is also consistent with the results of n- and p-type silicon nanowires measured between 75 and 325 K.[28]

We thank Patrick A. Lee and Z. Q. Zhang for discussions. This work is supported by HKUST through Contract No. RPC06/07.SC21. The computation resources were supported by the Shun Hing Education and Charity Fund. W.R. gratefully acknowledges the hospitality of Tomi Ohtsuki at Sophia University, Tokyo. Work at Ames Laboratory was supported by the U.S. Department of Energy, Basic Energy Sciences, including a grant of computer time at the NERSC in Berkeley under Contract No. DE-AC02-07CH11358.

*wren@ust.hk

[1] J. Y. Park, S. Rosenblatt, Y. Yaish, V. Sazonova, H. Ustunel, S. Braig, T. A. Arias, P. W. Brouwer, and P. L. McEuen, Nano Lett. **4**, 517 (2004).
[2] M. Gheorghe, R. Gutierrez, N. Ranjan, A. Pecchia, A. D. Carlo, and G. Cuniberti, Europhys. Lett. **71**, 438 (2005).
[3] W. Ren, J. R. Reimers, N. S. Hush, Y. Zhu, J. Wang, and H. Guo, J. Phys. Chem. C **111**, 3700 (2007).
[4] C. Z. Wang, C. T. Chan, and K. M. Ho, Phys. Rev. B **42**, 11276 (1990).
[5] C. Z. Wang, C. T. Chan, and K. M. Ho, Phys. Rev. B **39**, 8586 (1989).
[6] C. Z. Wang, C. T. Chan, and K. M. Ho, Phys. Rev. B **40**, 3390 (1989).
[7] C. H. Xu, C. Z. Wang, C. T. Chan, and K. M. Ho, J. Phys.: Condens. Matter **4**, 6047 (1992).
[8] M. S. Tang, C. Z. Wang, C. T. Chan, and K. M. Ho, Phys. Rev. B **53**, 979 (1996).
[9] W. Ren, J. Wang, and Z. Ma, Phys. Rev. B **72**, 195407 (2005).
[10] J. Kong, E. Yenilmez, T. W. Tombler, W. Kim, H. Dai, R. B. Laughlin, L. Liu, C. S. Jayanthi, and S. Y. Wu, Phys. Rev. Lett. **87**, 106801 (2001).
[11] C. Gomez-Navarro, P. J. D. Pablo, J. Gomez-Herrero, B. Biel, F. J. Garcia-Vidal, A. Rubio, and F. Flores, Nature Mater. **4**, 534 (2005).
[12] W. Ren and J. Wang, Phys. Rev. B **69**, 033306 (2004).
[13] T. Nakanishi and T. Ohtsuki, Physica B **249-251**, 801 (1998).
[14] S. Roche, J. Jiang, L. E. F. F. Torres, and R. Saito, J. Phys.: Condens. Matter **19**, 183203 (2007).
[15] L. E. F. Foa Torres, R. Avriller, and S. Roche, Phys. Rev. B **78**, 035412 (2008).
[16] L. E. F. Foa Torres and S. Roche, Phys. Rev. Lett. **97**, 076804 (2006).
[17] W. Ren, T. H. Cho, T. C. Leung, and C. T. Chan, Appl. Phys. Lett. **93**, 142102 (2008).
[18] B. L. Altshuler, JETP Lett. **41**, 648 (1985).
[19] P. A. Lee and A. D. Stone, Phys. Rev. Lett. **55**, 1622 (1985).
[20] H. Suzuura and T. Ando, Phys. Rev. Lett. **89**, 266603 (2002).
[21] N. E. Staley, C. P. Puls, and Y. Liu, Phys. Rev. B **77**, 155429 (2008).
[22] A. Fasolino, J. H. Los, and M. I. Katsnelson, Nature Mater. **6**, 858 (2007).
[23] T. Markussen, R. Rurali, A.-P. Jauho, and M. Brandbyge, Phys. Rev. Lett. **99**, 076803 (2007).
[24] M. Moško, P. Vagner, M. Bajdich, and T. Schäpers, Phys. Rev. Lett. **91**, 136803 (2003).
[25] M. S. Purewal, B. H. Hong, A. Ravi, B. Chandra, J. Hone, and P. Kim, Phys. Rev. Lett. **98**, 186808 (2007).
[26] C. L. Kane *et al.*, EPL **41**, 683 (1998).
[27] A. A. Kane, K. Loutherback, B. R. Goldsmith, and P. G. Collins, Appl. Phys. Lett. **92**, 083506 (2008).
[28] F. Vaurette, R. Leturcq, J. P. Nys, D. Deresmes, B. Grandidier, and D. Stievenard, Appl. Phys. Lett. **92**, 242109 (2008).